

# Direct observation of intrinsic Josephson junction characteristics in electron-doped $\text{Sm}_{2-x}\text{Ce}_x\text{CuO}_{4-\delta}$

Tsuyoshi Kawakami and Minoru Suzuki\*

*Department of Electronic Science and Engineering, Kyoto University, Kyotodaigaku-Katsura, Nishikyo-ku, Kyoto 615-8510, Japan*

(Received 14 October 2006; revised manuscript received 11 July 2007; published 3 October 2007)

We have investigated the current-voltage ( $CV$ ) characteristics of the intrinsic Josephson junctions (IJJs) in the electron-doped high- $T_c$  superconductor  $\text{Sm}_{2-x}\text{Ce}_x\text{CuO}_{4-\delta}$  by using a small mesa structure fabricated on a single crystal surface. It is found that multiple resistive branches, i.e., typical IJJ characteristics, are observed in the  $CV$  characteristics when the junction area of a mesa is  $10\ \mu\text{m}^2$  or less. It is also found that a typical Josephson critical current density  $J_c$  is  $7.5\ \text{kA}/\text{cm}^2$  at  $4.2\ \text{K}$  for  $T_c=20.7\ \text{K}$ . The Josephson penetration depth is experimentally estimated to be  $1.0\text{--}1.6\ \mu\text{m}$  from the size dependence of  $J_c$ . Both  $J_c$  and  $T_c$  are found to decrease with the carrier doping level, as is found for hole-doped  $\text{Bi}_2\text{Sr}_2\text{CaCu}_2\text{O}_{8+\delta}$  in the heavily overdoped region. These results are discussed in relation to the current locking in terms of the coupled Josephson junction stack model.

DOI: 10.1103/PhysRevB.76.134503

PACS number(s): 74.50.+r, 74.72.Jt

## I. INTRODUCTION

Due to its layered structure and large anisotropy, a crystal of a high- $T_c$  cuprate is generally regarded as a stack of tunnel Josephson junctions. These junctions are called intrinsic Josephson junctions (IJJs).<sup>1,2</sup> Since the IJJs are a crystal structure itself, the junction interfaces are atomically flat and clean, providing uniquely in high- $T_c$  superconductors almost ideal tunneling-type Josephson junction characteristics. With these characteristics, the IJJs are employed in a wide variety of researches such as those into the macroscopic quantum tunneling,<sup>3,4</sup> the interlayer tunneling spectroscopy,<sup>5,6</sup> collective vortex motion,<sup>7,8</sup> and others.<sup>9</sup>

The current-voltage ( $CV$ ) characteristics of the IJJs exhibit deep hysteresis and multiple resistive branches which correspond to the resistive states of the individual IJJs. Typical IJJ characteristics are usually observed in  $\text{Bi}_2\text{Sr}_2\text{CaCu}_2\text{O}_{8+\delta}$  (BSCCO), in which the IJJ characteristics were observed for the first time,<sup>1</sup> and in  $\text{Tl}_2\text{Ba}_2\text{Ca}_2\text{Cu}_3\text{O}_{10}$ ,<sup>2,10</sup> which has a crystal structure similar to BSCCO. These cuprates have a typical layered crystal structure and a significantly large anisotropy of  $\sim 100$  or greater.  $\text{Hg}_2\text{Ba}_2\text{Ca}_2\text{Cu}_3\text{O}_{10}$  has also a similar crystal structure and it was shown recently that this material also shows typical IJJ  $CV$  characteristics.<sup>11</sup>

On the other hand, in  $\text{YBa}_2\text{Cu}_3\text{O}_{7-x}$  (YBCO), which has a crystal structure with a moderate anisotropy, the IJJ characteristics were observed only for a limited number of samples, which have a small junction area and a low carrier doping level (underdoped).<sup>12-14</sup> In  $\text{RuSr}_2\text{GdCu}_2\text{O}_8$ , which is crystallographically analogous to YBCO, multiple resistive branches similar to those for YBCO were also observed in the  $CV$  characteristics.<sup>15</sup> For  $\text{La}_{2-x}\text{Sr}_x\text{CuO}_4$  crystals, multiple branches are not observed in the  $CV$  characteristics and the hysteresis is absent.<sup>16</sup> Thus  $CV$  characteristics of the IJJs are different among high- $T_c$  cuprates, depending on the crystal structure, the magnitude of its anisotropy, and the sample dimensions. The appearance and disappearance of the multiple resistive branches, which correspond to the switching of individual IJJs, are closely related to the current locking phe-

nomenon in a coupled Josephson junction stack.<sup>17</sup> The current locking is thought to occur through the inductive coupling between the junctions, that is, the Josephson coupling strength between the superconducting layers through the Josephson critical current density  $J_c$  and the penetration depth  $\lambda_J$ . Through  $J_c$ , on the other hand, the IJJ characteristics can be related to the inhomogeneity of the superconducting state, which is supposed recently.<sup>18-20</sup> Thus, the observation of the IJJ characteristics is important to understand the dynamics of a coupled Josephson junction array, and, in some cases, it is useful to probe into the inhomogeneous superconducting state of a cuprate.

Almost all the IJJ characteristics have been observed in hole-doped cuprates so far. Since the magnitudes of anisotropy and the Josephson plasma frequency for electron-doped cuprates are comparable with those for hole-doped cuprates, it is thought possible to observe the IJJ characteristics for electron-doped cuprates. In an earlier study, Schlenga *et al.*<sup>21</sup> observed the  $CV$  characteristics of the electron-doped high- $T_c$  superconductor  $\text{Pr}_{2-x}\text{Ce}_x\text{CuO}_{4+\delta}$  on a small platelet crystal. They observed the ac Josephson effect and several voltage steps in the  $CV$  characteristics, but not a multiple branch structure typical to IJJs. The present paper reports the direct observation of the IJJ characteristics and their multiple branch structure for the electron-doped cuprate  $\text{Sm}_{2-x}\text{Ce}_x\text{CuO}_{4-\delta}$  (SCCO) by using a small mesa structure fabricated on a single crystal surface. It is also found that the  $CV$  characteristics exhibit multiple resistive branches, only when the lateral mesa width is less than a few micrometers. This result indicates that the crystal structure of SCCO functions as superconductor-insulator-superconductor (SIS)-type IJJs like that of BSCCO. We discuss the relationship between the mesa size and the appearance of the multiple resistive branches in terms of the current locking phenomenon.

In the present study, several physical parameters have also been determined. A typical value for  $J_c$  is found to be approximately  $7.5\ \text{kA}/\text{cm}^2$  at  $4.2\ \text{K}$  for a SCCO mesa having a  $T_c$  of  $20.7\ \text{K}$ . From the size dependence of the Josephson critical current  $I_c$ , the value for  $\lambda_J$  is estimated to be  $1.0\text{--}1.6\ \mu\text{m}$ . This value is compared with the  $\lambda_J$  value calcu-

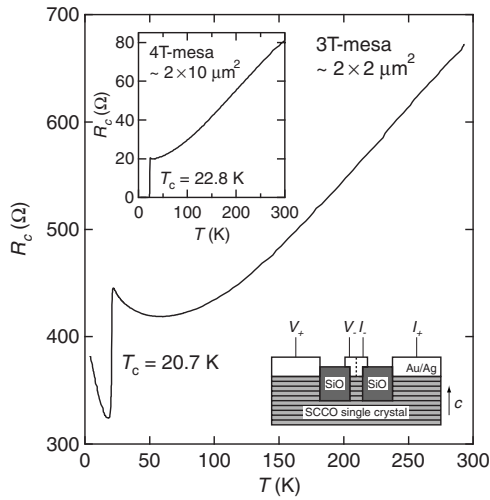


FIG. 1. Temperature dependence of the mesa resistance  $R_c$  for a SCCO 3T mesa  $2 \times 2 \mu\text{m}^2$  wide and 36 nm thick. Excitation current is  $1 \mu\text{A}$ . The top-left inset shows the  $T$  dependence of  $R_c$  for a SCCO 4T mesa  $2 \times 10 \mu\text{m}^2$  wide and 30 nm thick at an excitation current of  $5 \mu\text{A}$ . The bottom-right inset shows a schematic cross sectional view of the sample geometry (not to scale). For 4T mesas, a voltage terminal and a current terminal on top of a mesa are separated by a slit at the dashed line.

lated based on the coupled sine-Gordon equation. We also find that both  $J_c$  and  $T_c$  decreases monotonically with the carrier doping level. Finally, we discuss a possibility of the inhomogeneous superconducting state, which is suggested to exist in  $p$ -type cuprate superconductors.

## II. SAMPLE FABRICATION

SCCO single crystals employed were grown by the self-flux method<sup>22,23</sup> using a turnover technique, which provided platelike single crystals with flux-free shiny surfaces. As-grown crystals were first annealed in flowing Ar at  $945\text{--}950^\circ\text{C}$  for 15–20 h. Next, a Au(50 nm)/Ag(25 nm) double layer was evaporated on a crystal surface as a contact electrode, and then annealed in flowing Ar at  $400^\circ\text{C}$  for 5 min to reduce the contact resistance. From these crystals, small mesa structures, as shown in the inset to Fig. 1, were fabricated on top of a crystal surface using a standard photolithography and an Ar ion milling technique.<sup>5</sup> The mesa thickness, typically 30 nm, was controlled by the milling time. The electrode configuration we employed is either of a three-terminal (3T) type or of a four-terminal (4T) type. The size of the 3T mesas ranges from  $2 \times 2$  to  $10 \times 10 \mu\text{m}^2$  in area and 36 nm in height, while that of the 4T mesas, which have two electrodes on the top, is approximately  $2 \times 10 \mu\text{m}^2$  in area and 30 nm in height. These thicknesses of the mesas are much smaller than the averaged separation of the  $\text{Sm}_2\text{O}_3$  impurity-phase epitaxial stacking layers, which was reported to be several hundred nanometers.<sup>24</sup> This implies that the mesas in the present study contain no such impurity layers and that the properties observed are inherent to SCCO. Since the spacing of the  $\text{CuO}_2$  layers in SCCO is

0.60 nm, a mesa thickness of 30 nm corresponds to a stack of 50 IJJs.

## III. RESULTS

Figure 1 shows the temperature  $T$  dependence of the mesa resistance  $R_c$ , i.e., the  $c$ -axis resistance, for a typical 3T mesa. The resistive superconducting transition is seen at a midpoint  $T_c$  of 20.7 K. Residual resistance seen below  $T_c$  is the contact resistance, which corresponds to a contact resistivity of  $1 \times 10^{-5} \Omega \text{cm}^2$  near  $T_c$ . This is the smallest contact resistivity attained in the present study. The  $c$ -axis resistivity  $\rho_c$  of the mesa obtained from  $R_c$  is  $1.3 \Omega \text{cm}$  just above  $T_c$ , which is nearly equal to the value obtained from a  $\text{Nd}_{1.85}\text{Ce}_{0.15}\text{CuO}_4$  crystal.<sup>25</sup> The inset of Fig. 1 shows a typical  $T$  dependence of  $R_c$  for a 4T mesa. The  $\rho_c$  value near  $T_c$  obtained from this 4T mesa coincides with that for the 3T mesa. The metallic behavior of  $\rho_c$  seen in the wide temperature range is commonly seen in the  $n$ -type cuprates.<sup>22</sup>

Figures 2(a)–2(c) show the  $IV$  characteristics for three different kinds of SCCO mesas: a  $10 \times 10 \mu\text{m}^2$  3T mesa, a  $2 \times 2 \mu\text{m}^2$  3T mesa, and a  $2 \times 10 \mu\text{m}^2$  4T mesa. The samples in Figs. 2(b) and 2(c) are the same as those in Fig. 1. In Fig. 2(a), the  $IV$  curve exhibits neither hysteresis nor resistive branches, while in Fig. 2(b) the  $IV$  curve demonstrates small hysteresis and dozens of resistive branches. This is a typical difference seen in the  $IV$  characteristics when the mesas of different sizes are compared. Namely, the hysteresis and the resistive branches are observed when the mesa size is small. For 3T mesas, when the mesa area  $S$  is larger than a few  $\mu\text{m}^2$  but smaller than  $100 \mu\text{m}^2$ , the observed  $IV$  characteristics were occasionally intermediate ones between those in Fig. 2(a) and in Fig. 2(b). For example, the  $IV$  characteristics for a  $5 \times 5 \mu\text{m}^2$  3T mesa exhibited small hysteresis and several nonhysteretic step. From the  $S$  dependence of the  $IV$  characteristics for more than a dozen of small mesa samples, it is concluded that the multiple resistive branches are observed only when  $S$  is less than approximately  $10 \mu\text{m}^2$ .

In Fig. 2(c), on the other hand, the  $IV$  characteristics exhibit small hysteresis but no multiple resistive branches are seen. Although most of 4T mesas of the same size show similar  $IV$  characteristics, some of them occasionally exhibited a small steplike structure with an interval of 1–2 mV in the  $IV$  curve at low voltages. Similar  $IV$  characteristics were also observed for  $5 \times 5 \mu\text{m}^2$  3T mesas. The relationship between the shape of the  $IV$  characteristics and  $S$  also holds in this case, indicating that the shape of the  $IV$  characteristics depends primarily on the mesa area, irrespective of electrode configurations. When the depth of the hysteresis is defined as  $(I_c - I_r)/I_c$ , as described in Fig. 2(c), the hysteresis for  $2 \times 10 \mu\text{m}^2$  4T mesas ranged from 0% to 12%, as seen in the inset of Fig. 6(a). These values are significantly smaller than that of BSCCO, in which the hysteresis is much greater than 90%.

The dashed line in Fig. 2(c) corresponds to the resistance  $R_c$  at 24 K in the normal state. The  $IV$  curve approaches this line near  $\sim 40$  mV, which value is still much smaller than 300 mV, the product of the superconducting gap voltage of  $2\Delta/e = 6$  mV (Ref. 26) and the number of junctions  $N$  of 50.

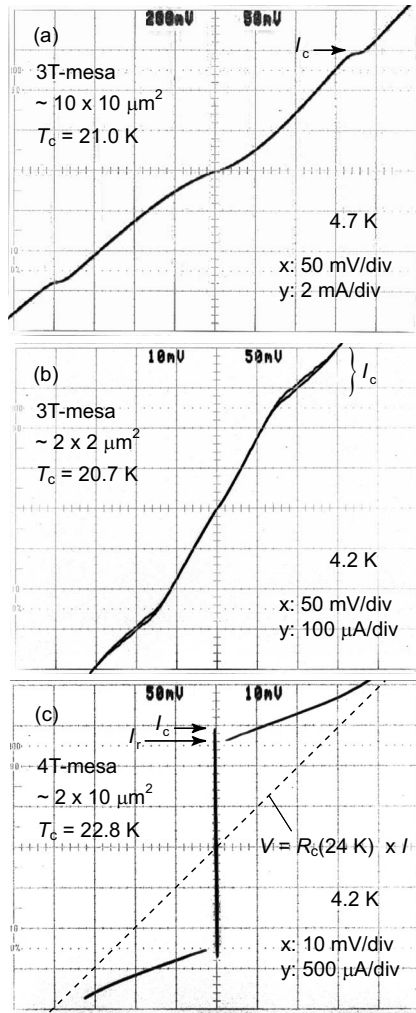


FIG. 2. *IV* characteristics for (a)  $10 \times 10 \mu\text{m}^2$  3T mesa, (b)  $2 \times 2 \mu\text{m}^2$  3T mesa, and (c)  $2 \times 10 \mu\text{m}^2$  4T mesa. The dashed line in (c) indicates the resistance of  $R_c = 20 \Omega$  at  $24 \text{ K}$ .  $I_r$  in (c) indicates the return current, below which the junction switches to the zero-voltage state.

Even if we take into account the fact that the interval of the resistive branches is usually much smaller than  $2\Delta/e$  by a factor of  $1/4$  to  $1/3$ , as in the case of the IJJs in BSCCO, the value of such is not sufficient to explain the above value of  $40 \text{ mV}$ . If we further take into account the presence of the pseudogap,<sup>27</sup> which causes an increase in the normal state resistivity by a factor of as large as 2 below  $T_c$ , then the inclination of the dashed line in Fig. 2(c) is reduced to its half and the *IV* characteristics may turn out consistent with the usual tunneling model. It is also conceivable that the IJJs in SCCO crystals are accompanied by a small amount of a shunting resistance, which also reduces the interval of the resistive branches. The *IV* characteristics in Fig. 2(c) can be partly explained in terms of such a shunting resistance.

Figure 3 shows an enlarged view of the *IV* characteristics in Fig. 2(b) in the positive voltage range for the  $2 \times 2 \mu\text{m}^2$  3T mesa at  $4.2 \text{ K}$ . In this measurement, an Ohmic resistive component comparable to the contact resistance was subtracted by using a differential circuitry. The distortion from

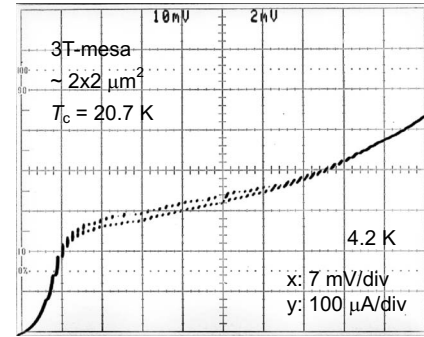


FIG. 3. The positive voltage part of the *IV* characteristics at  $4.2 \text{ K}$  for the  $2 \times 2 \mu\text{m}^2$  3T mesa in Fig. 2(b). The characteristics were observed by subtracting the Ohmic resistive component of  $250 \Omega$  using a differential circuitry to remove influence of the contact resistance.

the linearity near the origin (bottom-left corner) is due to the contact resistance. The *IV* characteristic shows clearly the resistive branches counting approximately 60, which coincides with  $N$ , the number of the IJJs in the mesa. This agreement indicates that these resistive branches derive from the IJJs naturally built in the SCCO crystal structure like in the case for *p*-type BSCCO, and not from epitaxial stacking faults such as  $\text{Sm}_2\text{O}_3$ .<sup>24</sup> The regular resistive branches are seen at a constant voltage interval  $V_c$  of  $1.0 \text{ mV}$ , which is by a factor of approximately  $1/6$  smaller than the superconducting gap  $2\Delta/e$  for *n*-type  $\text{Pr}_{1.85}\text{Ce}_{0.15}\text{CuO}_4$  and  $\text{Nd}_{1.85}\text{Ce}_{0.15}\text{CuO}_4$ .<sup>26</sup> Furthermore, the value for  $V_c/(2\Delta/e)$  is much smaller than that of  $\sim 1/3$  for BSCCO.<sup>28</sup> The depth of the hysteresis is  $10.3\%$  at the most, which value is significantly smaller than that for BSCCO. As for the maximum Josephson current  $I_c$  for individual junctions for the sample in Fig. 3, the values are distributed from  $150$  to  $450 \mu\text{A}$ . However, most of the junctions have an  $I_c$  of  $250$ – $350 \mu\text{A}$  in the  $10$ – $40 \text{ mV}$  range. These values are averaged to obtain the value of  $I_c = 300 \mu\text{A}$ . From this, the Josephson critical current density  $J_c = I_c/S$  is obtained to be approximately  $7.5 \text{ kA/cm}^2$  for this sample. The values for  $J_c$  were nearly the same for samples with similar  $S$  and  $T_c$  values. The above value is an order of magnitude larger than that of BSCCO (Ref. 29) and a factor of 2 larger than that of underdoped YBCO.<sup>14</sup>

The observed values of  $J_c$  for IJJs in SCCO lie between  $1.4 \text{ kA/cm}^2$  for slightly overdoped BSCCO (Ref. 29) at  $5 \text{ K}$  and  $26 \text{ kA/cm}^2$  for LSCO ( $x=0.09$ ) at  $4.2 \text{ K}$ .<sup>30</sup> A typical value for the Josephson plasma frequency  $\omega_p/2\pi$  for the *n*-type cuprates is  $230 \text{ GHz}$ , which lies between  $107 \text{ GHz}$  for BSCCO (Ref. 31) and  $600 \text{ GHz}$  for LSCO ( $x=0.10$ ).<sup>32</sup> These values are in qualitative agreement with the relationship  $\omega_p^2 = 2eI_c/\hbar C$ , where  $C$  is the capacitance of a junction, because if we assume that  $\epsilon/\epsilon_0 = 10$ , the values for  $\omega_p/2\pi$  are calculated to be  $135 \text{ GHz}$  for slightly overdoped BSCCO,  $200 \text{ GHz}$  for SCCO, and  $369 \text{ GHz}$  for LSCO ( $x=0.09$ ).

Figure 4 shows the  $T$  dependence of  $I_c$  for the  $2 \times 2 \mu\text{m}^2$  3T mesa shown in Fig. 3. The solid curve represents the theoretical  $I_c - T$  for a SIS Josephson junction based

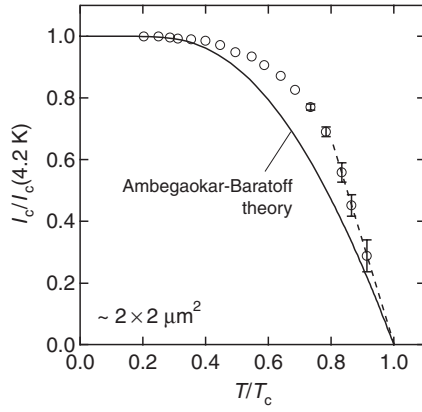


FIG. 4.  $T$  dependence of  $I_c$  for the  $2 \times 2 \mu\text{m}^2$  3T mesa in Fig. 3. Values for  $I_c$  were obtained from the 13th resistive branch. The solid curve represents the Ambegaokar-Baratoff theory. The dashed line are guides to the eyes.

on the Ambegaokar-Baratoff (AB) theory.<sup>33</sup> The overall behavior demonstrates qualitatively a feature characteristic to a SIS-type Josephson junction. However, a slight deviation from the AB theory is seen in the  $T/T_c$  range of 0.4–0.9. The upward deviation like this is also seen for slightly overdoped BSCCO.<sup>34</sup> This presents a contrast with the  $I_c-T$  data for  $\text{RuSr}_2\text{GdCu}_2\text{O}_8$ ,<sup>15</sup> underdoped  $\text{YBCO}$ ,<sup>13</sup> and  $\text{La}_{2-x}\text{Sr}_x\text{CuO}_4$ ,<sup>16</sup> in which only a little deviation is seen from the AB theory. The deviation of  $I_c-T$  from the theory may be related to the large junction effect at low temperatures. If the junction size is large compared with the Josephson penetration depth  $\lambda_J$ ,  $I_c$  is suppressed appreciably at low temperatures because  $\lambda_J$  decreases as  $T$  decreases. This is discussed later in relation to the Josephson critical current density  $J_c$ .

Figure 5 shows the  $S$  dependence of  $I_c$  at 4.2–5 K for mesas whose  $T_c$  is 20–21 K. It is clearly seen that the  $I_c$  data start to deviate from the linear relationship when  $S$  exceeds  $\sim 10 \mu\text{m}^2$ . This result indicates that the value for the Josephson penetration depth  $\lambda_J$  is estimated to be 1.0–1.6  $\mu\text{m}$ .<sup>35</sup> Thus, the  $I_c/S$  value obtained from a mesa of no larger than  $2 \times 10 \mu\text{m}^2$  provides a good estimate for  $J_c$ .

It is known that the  $c$ -axis conductivity at 300 K,  $\sigma_c$  (300 K), is nearly proportional to the doping level in a doping range centered at the optimal doping.<sup>18</sup> Therefore, it is considered that the  $\sigma_c$  (300 K) dependence represents the doping dependence. Figures 6(a) and 6(b) show the plots of  $J_c$  vs  $\sigma_c$  (300 K) and those for  $T_c$  vs  $\sigma_c$  (300 K), respectively, for  $2 \times 10 \mu\text{m}^2$  4T mesas and for  $2 \times 2 \mu\text{m}^2$  3T mesas. In the sense mentioned above, Fig. 6 represents the doping dependence of  $J_c$  and  $T_c$ . From these plots, it is seen that  $J_c$  and  $T_c$  decreases monotonically with increasing doping level.<sup>36</sup> This doping dependence presents a sharp contrast with those for the BSCCO system, in which  $J_c$  increases significantly with increasing doping. This is interpreted in terms of the doping level of the superconducting region in the electron-doped cuprate system.<sup>37</sup> The details are discussed in the following section.

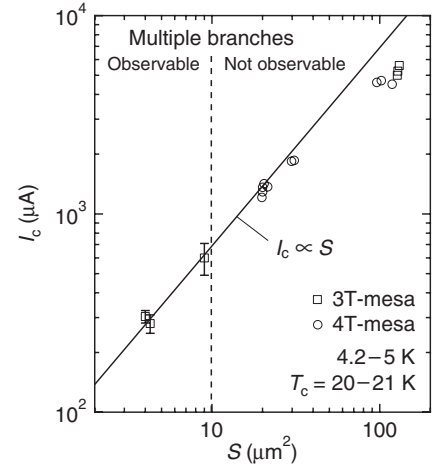


FIG. 5.  $S$  dependence of  $I_c$  for SCCO mesas with  $T_c = 20\text{--}21$  K. The  $I_c$  values were measured at 4.2–5 K. The solid line represents the proportionality relationship between  $I_c$  and  $S$ . The dashed line represents the boundary for the appearance of multiple resistive branches. In the left side of the border, plots for  $I_c$  have error bars due to different  $I_c$  values among multiple resistive branches. The  $S$  values of  $\sim 4$ ,  $\sim 9$ ,  $\sim 20$ ,  $\sim 30$ , and  $\sim 100 \mu\text{m}^2$  in the plot correspond to the junction dimensions of  $2 \times 2$ ,  $3 \times 3$ ,  $2 \times 10$ ,  $3 \times 10$ , and  $10 \times 10 \mu\text{m}^2$ , respectively.

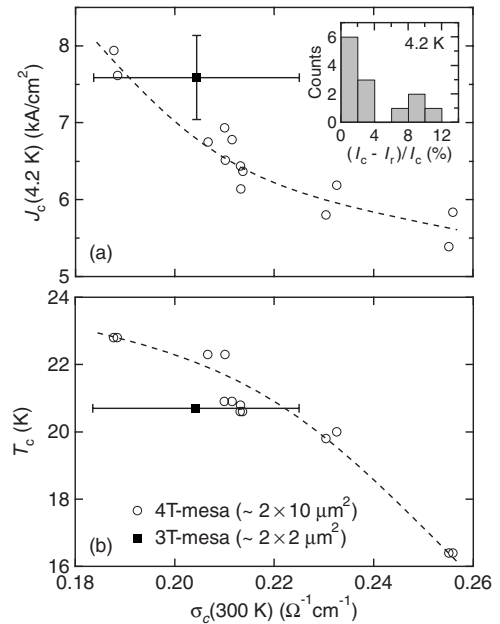


FIG. 6. Plots for (a)  $J_c$  (4.2 K) and (b)  $T_c$  as a function of  $\sigma_c$  (300 K). The filled symbols represent the data for the  $2 \times 2 \mu\text{m}^2$  3T mesa in Fig. 3, while the open symbols represent the data for  $2 \times 10 \mu\text{m}^2$  4T mesas. The  $\sigma_c$  (300 K) value for the 3T mesa is estimated by subtracting the extrapolated contact resistance at 300 K. The length of the vertical error bar represents the standard deviation of the  $J_c$  values. Dashed lines are guides to the eyes. The inset shows a histogram for the depth of hysteresis  $(I_c - I_r)/I_c$  at 4.2 K for the 4T mesas. The depth of hysteresis showed no clear correlation with  $T_c$ .

#### IV. DISCUSSION

##### A. Mesa size dependence of the intrinsic Josephson junction characteristics

In the present study, it is found that the multiple resistive branches are seen in the  $IV$  characteristic only when the mesa area is less than  $10 \mu\text{m}^2$ . It is known, on the other hand, that a mesa made of a BSCCO crystal shows multiple resistive branches with a large hysteresis in the  $IV$  characteristics even when the mesa is several tens of micrometer wide. The condition under which the multiple resistive branches are seen in the  $IV$  characteristics is related both to the presence of hysteresis and to the independent dynamic motion of each junction. If the  $IV$  characteristics exhibit no hysteresis or all the junctions are current locked and switch simultaneously, then the multiple resistive branches are not seen in the  $IV$  characteristics. In order to understand the present results, we need to rely on the following coupled sine-Gordon equation,<sup>38,39</sup> which describes the IJJs, as in Ref. 38.

$$\frac{d^2 \gamma_n}{d\xi^2} = \frac{L^2}{\lambda_m^2} j_{z,n} - \frac{L^2}{\lambda_k^2} (j_{z,n-1} + j_{z,n+1}) - \left( \frac{1}{\lambda_m^2} - \frac{2}{\lambda_k^2} \right) L^2 j_{\text{ext}},$$

$$\lambda_m^2 = \frac{\hbar}{2e\mu_0 t_{\text{eff}} J_c}, \quad \lambda_k^2 = \frac{\hbar}{2e\mu_0 d_{\text{eff}} J_c}, \quad (1)$$

where  $t_{\text{eff}} = t + 2\lambda \coth(d/\lambda)$ ,  $d_{\text{eff}} = \lambda / \sinh(d/\lambda)$ ,  $\lambda = d\lambda_{ab}/(d+t)$ ,  $t$  is the insulating layer thickness,  $d$  is the superconducting layer thickness,  $\gamma_n$  is the gauge-invariant phase between the  $(n-1)$ th and the  $n$ th superconducting layers,  $j_{z,n}$  is the current between the  $(n-1)$ th and the  $n$ th superconducting layers normalized by  $J_c$ ,  $L$  is the dimension of the junction along the  $x$  axis,  $\xi = x/L$  is the normalized coordinate, and other notations are the same as in Ref. 38.

The coupling strength between adjacent junctions is determined by the second term in the right hand side of Eq. (1). Therefore, the ratio of the junction length  $L$  to  $\lambda_k$  determines the behavior of the dynamic motion. When  $d, t \ll \lambda$ , the relationship  $\lambda_m \approx \lambda_k$  holds. In this case, the Josephson penetration depth  $\lambda_J$  is equal to  $\lambda_m$ . From this relationship, it follows that when the ratio  $L/\lambda_k$  is larger than a certain value, all the junctions switch to the voltage state simultaneously, namely, the current locking (CL) phenomenon manifests itself. As numerically demonstrated by Goldobin and Ustinov,<sup>17</sup> this CL is a dynamic phenomenon brought about by the inductive coupling of long Josephson junctions. This is also supported experimentally on double junctions.<sup>40</sup> It is known that the IJJ resistive branches are observed for BSCCO in a much larger mesa sample than for SCCO. This fact implies that the value of  $\lambda_k$  for BSCCO is larger than that for SCCO. This is easily confirmed; if we use the values of  $\lambda_{ab} = 170 \text{ nm}$ ,<sup>41</sup>  $t = 1.2 \text{ nm}$ ,  $d = 0.3 \text{ nm}$ , and  $J_c = 500 \text{ A/cm}^2$ , we obtain the value of  $\lambda_k = 3.7 \mu\text{m}$  for BSCCO, while if we use the values of  $\lambda_{ab} = 150 \text{ nm}$ ,<sup>42</sup>  $t = 0.45 \text{ nm}$ ,  $d = 0.15 \text{ nm}$ , and  $J_c = 7500 \text{ A/cm}^2$ , we obtain the value of  $\lambda_k = 0.68 \mu\text{m}$  for SCCO. Thus,  $\lambda_k$  for SCCO is much smaller than that for BSCCO, so that the CL takes place in the IJJs of SCCO more easily than in BSCCO.

McCumber's parameter is represented by  $\beta_c = 2eI_c R^2 C / \hbar = 2eJ_c \rho_c^2 \varepsilon_0 \varepsilon_r (t+d)^2 / \hbar t$ . If we use the values of  $\rho_c = 1.33 \Omega \text{ cm}$ ,  $\varepsilon_r = 10$ ,  $J_c = 7.5 \times 10^3 \text{ A/cm}^2$ ,  $t = 0.45 \text{ nm}$ , and  $d = 0.15 \text{ nm}$ , then we obtain  $\beta_c = 2.86$  for SCCO. Therefore, we can expect a small hysteresis in the  $IV$  characteristics of IJJs in SCCO. However, this value is larger than 1 by only a small amount so that it can change to less than 1 when  $\rho_c$  or  $J_c$  is decreased appreciably. The vicinity of  $\beta_c$  to 1 reflects the occasional disappearance of the hysteresis in the SCCO  $IV$  characteristics in the present experiments. On the other hand, it is easily seen that  $\beta_c > 100$  for BSCCO and a large hysteresis is always expected in the  $IV$  characteristics of BSCCO IJJs. Since  $\beta_c$  is a parameter reflecting the capacitance of a Josephson junction, a large value for  $\beta_c$  probably favors the individual switching, where the charge is dynamically induced in the thin superconducting layers in the voltage state. It may be related to the fact that the multiple branch  $IV$  characteristics can be observed even in BSCCO mesas whose size is much larger than  $\lambda_J$ .

In the model described by Eq. (1),  $\lambda_m$  corresponds to  $\lambda_J$ , the Josephson penetration depth for a single junction. It is easily seen that  $\lambda_m \approx \lambda_J$  and  $1/\lambda_k \approx 0$  when  $d \gg \lambda$ . In the present case,  $d \ll \lambda$ , so that it holds that  $\lambda_J \approx \lambda_m \approx \lambda_k = 0.68 \mu\text{m}$  for SCCO using the values of  $\lambda_{ab} = 150 \text{ nm}$  and  $J_c = 7500 \text{ A/cm}^2$ . This value is smaller than the experimental value of  $1.0\text{--}1.6 \mu\text{m}$  obtained from the  $S$  dependence of  $I_c$  by a factor of approximately 0.5. This may leave a possibility that the  $T$  dependence of  $I_c$  is influenced from the large junction effect, in which  $I_c$  is suppressed at low temperatures.

##### B. Doping dependence of $J_c$

As shown in Fig. 6(a), it is found that  $J_c$  decreases with increasing carrier doping level. According to the AB theory,<sup>33</sup>  $J_c = \pi\Delta/2eR_N$  at  $T=0$ , where  $R_N$  is the normal tunneling resistance per unit area per junction. In the present study,  $R_N$  is nearly proportional to  $\rho_c$ , so that Fig. 6(a) combined with the AB theory implies that  $\Delta$  decreases with increasing doping level. Since Fig. 6(b) indicates a decrease in  $T_c$ , the concomitant behavior of  $\Delta$  and  $T_c$  is reasonable in light of the BCS theory. All these behaviors imply that the superconducting SCCO system is in the overdoped region. On the other hand, if we estimate the value for  $J_c$  using the values of  $2\Delta = 6 \text{ meV}$ ,  $R_N S = 1.5 \Omega$ ,  $S = 2 \times 3 \mu\text{m}^2$  ( $\rho_c = 1 \Omega \text{ cm}$ ), we obtain  $J_c = 7.85 \times 10^4 \text{ A/cm}^2$ , which is an order of magnitude larger than the observed value. The large difference between the AB theory and the experimental data as in the present study is also observed in the BSCCO system,<sup>18,19</sup> and is arguably regarded as evidence for the inhomogeneous superconducting state, where superconducting regions and nonsuperconducting ones are separated spatially on a fine scale. As in the underdoped BSCCO system, the present data may indicate the existence of the inhomogeneous superconducting state in the electron-doped SCCO system, even though the SCCO samples are in the overdoped region,<sup>37</sup> like in an overdoped BSCCO system, where inhomogeneous superconducting state is supposed to exist.<sup>43</sup> However, if we take into account that the present  $J_c$  values for the overdoped SCCO system are more than 2 orders of

magnitude larger than the  $J_c$  values for the underdoped BSCCO system, the above scenario needs further study to be convincing, in particular, on the doping dependence of  $J_c$ . A discrepancy of 1 order of magnitude in  $J_c$  can be accounted for in terms of different origins, which may include the large junction effect,  $d$ -wave symmetry of the superconducting order parameter, and others.<sup>44,45</sup>

## V. CONCLUSIONS

We have observed the IJJ characteristics in the  $n$ -type SCCO system by using a small thin mesa structure. It is found that the multiple resistive branches, which reflects the individual switching of SIS-type IJJs, are observed in the  $IV$  characteristics only when the mesa area is below  $10 \mu\text{m}^2$ . From the  $S$  dependence of  $I_c$ ,  $\lambda_J$  is estimated to be  $1\text{--}1.6 \mu\text{m}$ , which is compared with the theoretical estimate

of  $0.68 \mu\text{m}$ . In comparison with the case for the IJJs in the BSCCO system, it is found that the coupling strength of the IJJs in the SCCO system is greater than that in the BSCCO system. It is also found that  $J_c$  is approximately  $7.5 \text{ kA/cm}^2$  at  $4.2 \text{ K}$  for a  $2 \times 2 \mu\text{m}^2$   $3\text{T}$  mesa with a  $T_c$  of  $20.7 \text{ K}$ . Both  $J_c$  and  $T_c$  are found to decrease with the carrier doping level, a behavior similar to the case for  $p$ -type BSCCO in the heavily overdoped region. The observed value for  $J_c$  is found to be an order of magnitude smaller than the theoretical estimate, which is indicative of the existence of the inhomogeneous superconducting state as a possible origin.

## ACKNOWLEDGMENTS

The authors acknowledge useful discussions with T. Shibauchi. This work was partially supported by the 21st Century COE Program (Grant No. 14213201). T.K. was supported by the JSPS.

\*Corresponding author; suzuki@kuee.kyoto-u.ac.jp

- <sup>1</sup>R. Kleiner, F. Steinmeyer, G. Kunkel, and P. Müller, Phys. Rev. Lett. **68**, 2394 (1992).
- <sup>2</sup>R. Kleiner and P. Müller, Phys. Rev. B **49**, 1327 (1994).
- <sup>3</sup>K. Inomata, S. Sato, K. Nakajima, A. Tanaka, Y. Takano, H. B. Wang, M. Nagao, H. Hatano, and S. Kawabata, Phys. Rev. Lett. **95**, 107005 (2005).
- <sup>4</sup>X. Y. Jin, J. Lisenfeld, Y. Koval, A. Lukashenko, A. V. Ustinov, and P. Müller, Phys. Rev. Lett. **96**, 177003 (2006).
- <sup>5</sup>M. Suzuki, T. Watanabe, and A. Matsuda, Phys. Rev. Lett. **82**, 5361 (1999).
- <sup>6</sup>V. M. Krasnov, A. Yurgens, D. Winkler, P. Delsing, and T. Claesson, Phys. Rev. Lett. **84**, 5860 (2000).
- <sup>7</sup>S. Ooi, T. Mochiku, and K. Hirata, Phys. Rev. Lett. **89**, 247002 (2002).
- <sup>8</sup>M. Tachiki, M. Iizuka, K. Minami, S. Tejima, and H. Nakamura, Phys. Rev. B **71**, 134515 (2005).
- <sup>9</sup>A. A. Yurgens, Supercond. Sci. Technol. **13**, R85 (2000).
- <sup>10</sup>K. Schlenga, G. Hechtfisher, R. Kleiner, W. Walkenhorst, P. Müller, H. L. Johnson, M. Veith, W. Brodkorb, and E. Steinbeiß, Phys. Rev. Lett. **76**, 4943 (1996).
- <sup>11</sup>A. Ogawa, T. Sugano, H. Wakana, A. Kamitani, S. Adachi, Y. Tarutani, and K. Tanabe, Jpn. J. Appl. Phys., Part 2 **43**, L40 (2004).
- <sup>12</sup>M. Rapp, A. Murk, R. Semerad, and W. Prusseit, Phys. Rev. Lett. **77**, 928 (1996).
- <sup>13</sup>H. B. Wang, J. Chen, K. Nakajima, Y. Yamashita, P. H. Wu, T. Nishizaki, K. Shibata, and N. Kobayashi, Phys. Rev. B **61**, R14948 (2000).
- <sup>14</sup>M. Nagao, T. Kawae, K. S. Yun, H. B. Wang, Y. Takano, T. Hatano, T. Yamashita, M. Tachiki, and H. Maeda, J. Appl. Phys. **98**, 073903 (2005).
- <sup>15</sup>T. Nachtrab, D. Koelle, R. Kleiner, C. Bernhard, and C. T. Lin, Phys. Rev. Lett. **92**, 117001 (2004).
- <sup>16</sup>Y. Mizugaki, Y. Uematsu, S. J. Kim, J. Chen, K. Nakajima, T. Yamashita, H. Sato, and M. Naito, J. Appl. Phys. **94**, 2534 (2003).
- <sup>17</sup>E. Goldobin and A. V. Ustinov, Phys. Rev. B **59**, 11532 (1999).
- <sup>18</sup>Y. Yamada, K. Anagawa, T. Shibauchi, T. Fujii, T. Watanabe, A. Matsuda, and M. Suzuki, Phys. Rev. B **68**, 054533 (2003).
- <sup>19</sup>M. Suzuki, T. Hamatani, Y. Yamada, K. Anagawa, and T. Watanabe, IEEE Trans. Appl. Supercond. **15**, 189 (2005).
- <sup>20</sup>Y. Yamada and M. Suzuki, Phys. Rev. B **74**, 054508 (2006).
- <sup>21</sup>K. Schlenga, W. Biberacher, G. Hechtfisher, R. Kleiner, B. Schey, O. Waldmann, W. Walkenhorst, P. Müller, F. X. Regi, H. Savary, J. Schneck, M. Brinkmann, H. Bach, K. Westerholt, and G. Winkel, Physica C **235-240**, 3273 (1994).
- <sup>22</sup>Y. Hidaka and M. Suzuki, Nature (London) **338**, 635 (1989).
- <sup>23</sup>J. L. Peng, Z. Y. Li, and R. L. Greene, Physica C **177**, 79 (1991).
- <sup>24</sup>P. K. Mang, S. Larochele, A. Mehta, O. P. Vajk, A. S. Erickson, L. Lu, W. J. L. Buyers, A. F. Marshall, K. Prokes, and M. Greven, Phys. Rev. B **70**, 094507 (2004).
- <sup>25</sup>H. J. Kang, P. Dai, J. W. Lynn, M. Matsuura, J. R. Thompson, S. C. Zhang, D. N. Argyriou, Y. Onose, and Y. Tokura, Nature (London) **423**, 522 (2003).
- <sup>26</sup>S. Kleefisch, B. Welter, A. Marx, L. Alff, R. Gross, and M. Naito, Phys. Rev. B **63**, 100507(R) (2001).
- <sup>27</sup>T. Kawakami, T. Shibauchi, Y. Terao, M. Suzuki, and L. Krusin-Elbaum, Phys. Rev. Lett. **95**, 017001 (2005).
- <sup>28</sup>M. Suzuki, T. Watanabe, and A. Matsuda, IEEE Trans. Appl. Supercond. **9**, 4507 (1999).
- <sup>29</sup>M. Suzuki, T. Watanabe, and A. Matsuda, Phys. Rev. Lett. **81**, 4248 (1998).
- <sup>30</sup>Y. Y. Uematsu, N. Sasaki, Y. Mizugaki, K. Nakajima, T. Yamashita, S. Watauchi, and I. Tanaka, Physica C **362**, 290 (2001).
- <sup>31</sup>T. Ichiguchi, Physica C **293**, 105 (1997).
- <sup>32</sup>H. Shibata and T. Yamada, Physica C **293**, 191 (1997).
- <sup>33</sup>V. Ambegaokar and A. Baratoff, Phys. Rev. Lett. **10**, 486 (1963).
- <sup>34</sup>M. Suzuki, T. Watanabe, and A. Matsuda, IEEE Trans. Appl. Supercond. **9**, 4511 (1999).
- <sup>35</sup>We employ a linear current-phase model of Barone *et al.* (Refs. 46 and 47), in which the Josephson current  $J_c \sin \varphi$  is approximated by  $J_c \chi \varphi$ , where  $\chi = 1/2$ . When the Josephson current flows perpendicular to the junction plane, this equation

together with the Maxwell equation leads to the ratio of the critical current to the junction area  $I_c/S = (4\alpha\beta J_c \lambda_J^2 / ab\chi^2) \tanh(a\chi/2\alpha\lambda_J) \tanh(b\chi/2\beta\lambda_J)$ , where  $a$  and  $b$  are the side lengths of a rectangular junction,  $S=ab$ ,  $\alpha$  and  $\beta$  are constants with  $\alpha^{-2} + \beta^{-2} = 1$ . For a square junction, where  $a=b$  and  $\alpha=\beta$ ,  $I_c/S=0.9$  when  $a/4\sqrt{2}\lambda_J=0.4$ , leading to an estimate of  $\lambda_J=1.4 \mu\text{m}$  when  $S=10 \mu\text{m}^2$ . For a rectangular junction, where we assume that  $|H_x/H_y|=a/b$  at corners  $(\pm a/2, \pm b/2)$ , then  $\alpha/\beta=a/b$  and  $I_c/S=0.9$  when  $\sqrt{ab}/4\sqrt{\alpha\beta}\lambda_J=0.4$ , leading to an estimate of  $\lambda_J=1.22 \mu\text{m}$  when  $S=2 \times 10 \mu\text{m}^2$  as reflected in Fig. 5. In the case of in-line type current flow,  $I_c/S$  starts to deviate when  $b$  is  $2\lambda_J$  (Ref. 46), leading to an estimate of  $\lambda_J=1.58 \mu\text{m}$  when  $a=b=\sqrt{10} \mu\text{m}^2$ , or an estimate of  $\lambda_J=1.0 \mu\text{m}$  when  $a=10 \mu\text{m}$  and  $b=2 \mu\text{m}$ . Thus, the result in Fig. 5 gives an estimate of  $\lambda_J=1.0-1.6 \mu\text{m}$ .

<sup>36</sup>In Fig. 6, the data for the  $2 \times 2 \mu\text{m}^2$  3T mesa are also plotted, showing a slight deviation from the relationship for the 4T mesas. If we take into account the error due to the contact resistance, it is reasonably thought that the data for 3T mesas also fall on the same relationship.

- <sup>37</sup>T. Kawakami, T. Shibauchi, Y. Terao, and M. Suzuki, Phys. Rev. B **74**, 144520 (2006).  
<sup>38</sup>R. Kleiner, P. Müller, H. Kohlstedt, N. F. Pedersen, and S. Sakai, Phys. Rev. B **50**, 3942 (1994).  
<sup>39</sup>S. Sakai, P. Bodin, and N. F. Pedersen, J. Appl. Phys. **73**, 2411 (1993).  
<sup>40</sup>H. Yamamori, A. Fujimaki, Y. Takai, and H. Hayakawa, Jpn. J. Appl. Phys., Part 2 **33**, L846 (1994).  
<sup>41</sup>M. Däumling and G. V. Chandrasekhar, Phys. Rev. B **46**, 6422 (1992).  
<sup>42</sup>L. Fàbrega, J. Fontcuberta, B. Martínez, and S. Piñol, Phys. Rev. B **50**, 3256 (1994).  
<sup>43</sup>K. Anagawa, T. Watanabe, and M. Suzuki, Phys. Rev. B **73**, 184512 (2006).  
<sup>44</sup>S. Kashiwaya and Y. Tanaka, Rep. Prog. Phys. **63**, 1641 (2000).  
<sup>45</sup>K. Maki and S. Haas, Phys. Rev. B **67**, 020510 (2003).  
<sup>46</sup>A. Barone and G. Paternó, *Physics and Applications of the Josephson Effect* (Wiley, New York, 1982).  
<sup>47</sup>A. Barone, W. J. Johnson, and R. Vaglio, J. Appl. Phys. **46**, 3628 (1975).